

Uniaxial Compaction Behavior of Filled Polymer Powders

S. K. BHATEJA and J. R. GILBERT, *Electronic and Information Sector, 3M / 3M Center, 236-1B-15, St. Paul, Minnesota 55144* and
E. H. ANDREWS, *Department of Materials, Queen Mary College, University of London, London, England E1 4NS*

Synopsis

A simple method is described to obtain rheological data on filled polymeric materials in the form of powders. The powder is compacted in a cylindrical chamber by a plunger driven by the cross-head in an Instron testing machine and the load-displacement curve is recorded. Further information is obtained by compressing the powder to a fixed load and measuring the load decay with time (stress-relaxation). The tests are illustrated by application to "monocomponent toner" powders used in dry copying or nonimpact printing processes. It is shown that compaction and stress-relaxation data are able to differentiate between different toners and facilitate the prediction of their relative performances in terms of pressure fusing. A mechanical spring-dashpot-slider model is effective in describing the rheological behavior of these powders and its dependence on the loading of a hard filler (magnetic pigment). The latter affects the "slider" yield stress in the model but has no influence on the relaxation times.

INTRODUCTION

Much work has been done to characterize and explain the rheological behavior of solid polymers and polymer melts. Polymer solutions and particulate suspensions have also received attention and these subjects are covered in a wide range of textbooks.

There are, however, situations in which polymeric materials are used (in their final application) in the form of powders, and there appears to be very little information available on the rheological behavior of polymers in this form. A case of particular interest and practical importance is that of "monocomponent toner" powders used in nonimpact printing or copying processes.

Monocomponent toners consist of small particles of polymer and/or polymeric wax, typically 5 to 50 μm in diameter, in which are embedded much smaller magnetic pigment particles (typically 0.3–0.5 μm in average size). Typically, in order to improve their flow character, the toner particles are "spheroidized" and surface blended with a flow agent such as silica.

In use, the magnetic character of the toner particles facilitates their retention on the developer roll (fed by the toner hopper), their development onto the charged areas of a photoconductor drum (constituting the latent "image" to be copied or printed) and their subsequent transfer to a paper surface. Once the powder image has been placed on paper, it has to be "fused" or fixed in place to form a permanent image. A typical nonimpact printing process (electrophotographic) is shown schematically in Figure 1.

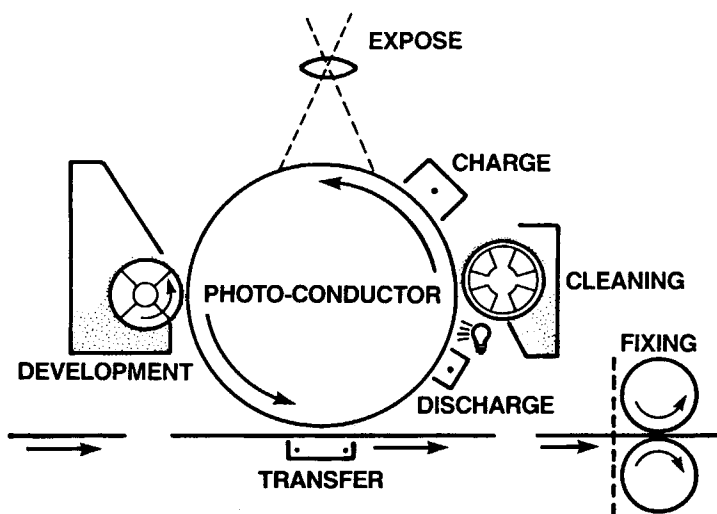


Fig. 1. A schematic diagram showing electrophotographic copying/printing process.

The final image-fusing process is the one that makes use of the rheology of the toner powder and thus of the polymeric material of which it is composed. Two methods are commonly employed for fusing/fixing toned images onto paper, namely, pressure fusing and heat fusing. In the first, the polymer particles are mechanically squashed onto the paper surface by passing the paper between fusing rollers. In the second, the particles are "melted" by thermal irradiation or conduction and intimate (permanent) contact with the paper is achieved by fluid flow. Clearly, different particle rheologies are needed for the two different "fusing" methods.

Fusing obviously involves either melt flow or plastic flow under pressure, but in the latter case it also involves strain recovery processes. This follows because a particle squashed onto a surface by applied pressure may partially recover its shape when the pressure is released (see Fig. 2). Thus, referring to Figure 3, stress-strain behavior Ia is preferable to behavior Ib for a pressure fusing toner material.

In this paper, we describe experiments designed to provide some basic rheological information about monocomponent toner powders, especially suited for their pressure-fusing behavior. The materials used were either commercial or 3M experimental toner powders and two kinds of test were carried out. In

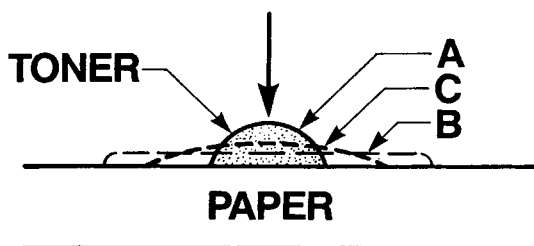


Fig. 2. Schematic diagram showing deformation of the toner particles in the imaged area before, during and after passing through the fuser nip.

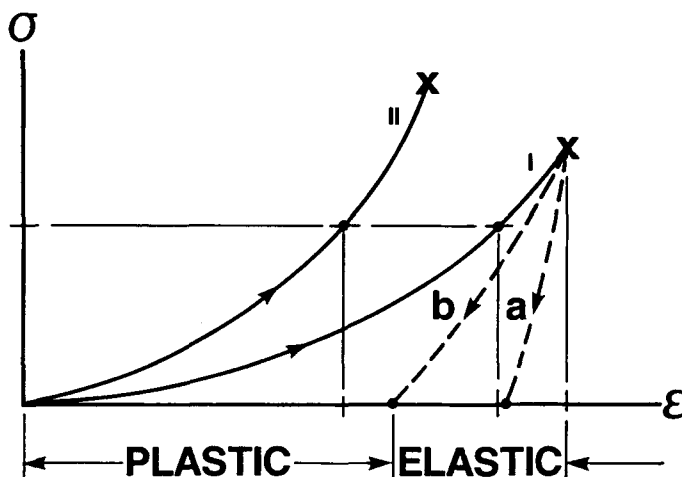


Fig. 3. Schematic axial load-displacement curves during loading and unloading of various toners showing elastic and plastic deformation.

the first, compaction test, we ascertain the resistance of toners to plastic deformation under pressure, while in the second, stress-relaxation test, we measure the powder's capacity to store elastic energy and thus its tendency to recover shape when load is released. These two simple tests, especially when carried out as a function of pigment loading, provide an excellent method for comparing different toners. They should also help us construct quantitative models of the pressure-fusing process. We are not concerned here directly with the heat-fusing process, but one heat-fusing toner has been included (Table I) for comparison and interest.

EXPERIMENTAL

Materials

The five toners examined in the present paper along with some of their characterization data such as the particle size distribution (PSD), the glass

TABLE I
Toners Examined Along with Some of Their Nonfunctional Data

Toner Sample #	Type	Magnetic pigment loading (wt%)	PSD (μm)	DSC		
				T_g ($^{\circ}\text{C}$)	T_m ($^{\circ}\text{C}$)	h_f (Cal/g)
A	Heat-fusing	60	8-12-20 ^a	70	—	—
B	Pressure-fusing	60	10-25-45	—	110.4	23.2
C	Pressure-fusing	60	8-12-20	—	107.6	18.7
D	Pressure-fusing	35	6-10-16	—	123.7	27.4
E	Pressure-fusing	60	11-20-40	—	124	18.6

^aPSD of 8-12-20 μm implies: 5% of the toner particles (by volume) $\leq 8 \mu\text{m}$; 50% of the particles = 12 μm ; 95% of the particles $\leq 20 \mu\text{m}$.

transition temperature (T_g), peak melting temperature (T_m), and the heat of fusion (h_f), as measured by the differential scanning calorimeter (DSC) technique are listed in Table I. The heat-fusing toner (A) contains a polyester base resin, while all the pressure-fusing toners either have a matrix of a high density polyethylene wax alone or in combination with a low density polyethylene wax. In addition to these five toners, some stress-relaxation measurements were also made on three other experimental toners of type C, in which, keeping everything else as constant as possible, the magnetic pigment loading was varied from 35 to 65 wt%.

TONER COMPACTION EXPERIMENTS

The toner powders were compacted in a 0.35 in. diameter \times 0.75 in. long cylindrical cavity in an Instron testing machine using a steel plunger in two different types of tests. In one test (the stress-strain test), the toner powders were compacted at a constant deformation rate of 1 in./min and the compressive axial load-displacement behavior was monitored continuously during compaction. In the other test (the stress-relaxation test), the toner powders were compressed at a constant deformation rate of 1 in./min to an arbitrary load of 200 lb., the Instron cross-head was stopped and the stress was observed to relax as a function of time. Although the initial rate of loading in a stress-relaxation test is supposed to be instantaneous (or at least extremely fast), any attempts in the present test to increase the deformation rate beyond 1 in./min resulted in the toner powder squirting out from the clearance along the chamber walls.

RESULTS AND DISCUSSION

Uniaxial Compressive Stress-Strain Behavior of Different Toners

Figure 4 compares the axial load-axial displacement behavior of the four pressure-fusing toners with that of the heat-fusing toner (toner A). These data clearly show that there are significant differences between different toners. This is especially true in view of the small magnitude of the experimental scatter in data shown in Figure 5, which shows the axial load-displacement curves obtained on five different but identical runs made on one given toner (C). Thus, not only can this test distinguish the heat-fusing toner from the four pressure-fusing toners, it can also differentiate between the different pressure-fusing toners. The significance of the test can be seen, at least qualitatively, from Figure 3, which shows schematically the axial load-displacement response of two different toners. Toner I shows a better potential for pressure fixing than does toner II, because at a given load/stress level, it deforms much more than toner II. However, as already indicated, this information needs to be combined with the "unloading" data before conclusions can be drawn about the pressure-fusing capabilities of a given toner. Figure 2 shows schematically what happens to the toner particles in the imaged area as they pass through the fuser nip. When the toner heap in the image area (position A) experiences the applied pressure, it gets flattened/deformed (position B). However, as the image leaves the nip area, the elastic part of the

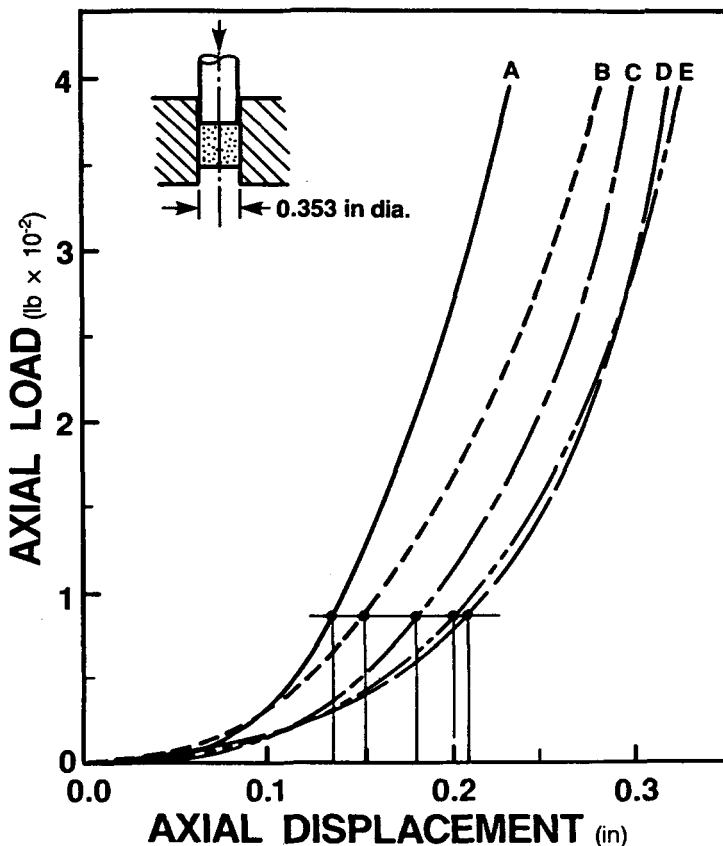


Fig. 4. Axial load-axial displacement curves for the five different toners.

deformation is recovered; the only permanent deformation that remains in the fused image is the plastic deformation (position C). Thus, of the two toners of Figure 3, both of which follow curve I during loading, the one that follows curve "a" during unloading shows better potential for pressure-fixing than the one that follows curve "b." Of course, the data presented in Figure 4 do not include the unloading response. However, based on the loading response alone, there are significant differences between the two categories (heat- vs. pressure-fusing) of toners as well as between different toners in the pressure-fusing category.

The deformation or degree of compaction obviously depends, at a given load, upon the yield stress of the polymer, plus any strain hardening that may occur. Yield stress, in turn, should depend upon the temperature relative to T_g or T_m of the polymer or wax. Figure 6 shows the axial displacement at an arbitrary load of 0.008 lb. for the five toners tested and plotted against T_g or T_m . There is indeed a correlation, but it goes the wrong way, the higher melting point materials (lower relative temperature of experiment) giving the larger deformations, not the smaller as expected. It is clear, therefore, that factors other than relative temperature are involved in determining the deformability of these powders. Obvious factors include the filler (pigment)

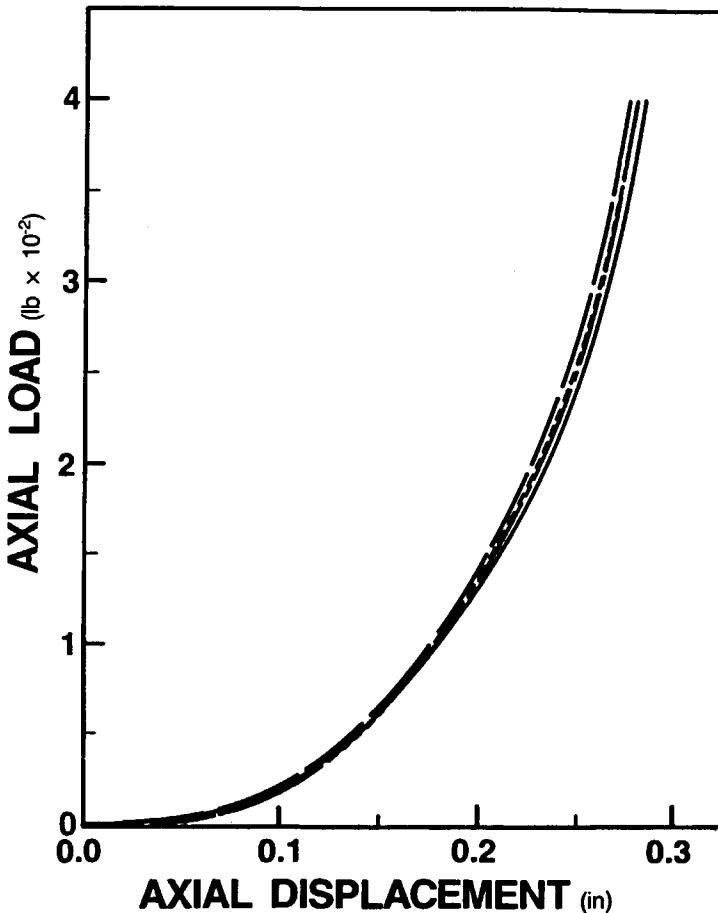


Fig. 5. Axial load-displacement curves for five different samples of toner C showing experimental scatter in data.

concentration, the presence of silica added to improve flow, particle size and distribution, etc. It is also not totally clear how any "structure" in the powder influences these results. Such factors as particle size distribution, nonsphericity of particles, particle catenation (chain formation) will all affect the compressibility of the powder. However, it will be seen in the next section that the stress-relaxation test ranks the five toners in virtually the same order as the uniaxial compression tests (the most compliant powder has the greatest stress-relaxation). This strongly suggests that the compressive behavior is dominated by particle rheology rather than interparticulate effects.

STRESS-RELAXATION BEHAVIOR

The five different toners of Figure 4 were loaded in uniaxial compression to 200 lb. load and their stress-relaxation behavior was monitored and is shown in Figure 7. Again, there are significant differences between the stress-relaxation behavior of the five different toners, which rank in the same order as the axial load-displacement curves of Figure 4. Typically, all toners show the

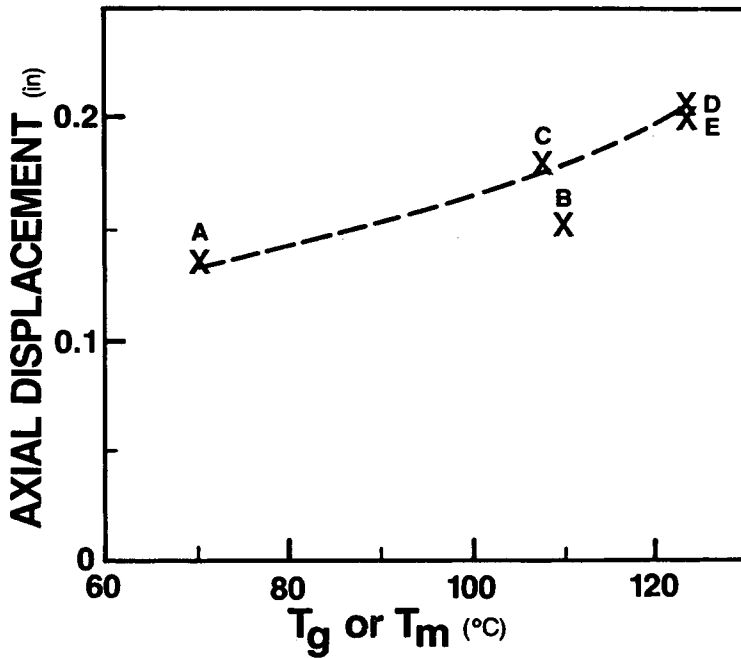


Fig. 6. Variation of axial displacement at a fixed load vs. T_m or T_g for the five different toners.

elastic (instantaneous) response, the delayed-elastic response and flow manifested by the stress relaxing to a certain yield value, Y . Some interesting features of these data became apparent when an attempt was made to analyze these data in terms of the spring-dashpot-slider mechanical models employed for describing the response of polymer melts containing high loadings of inorganic fillers.⁹⁻¹²

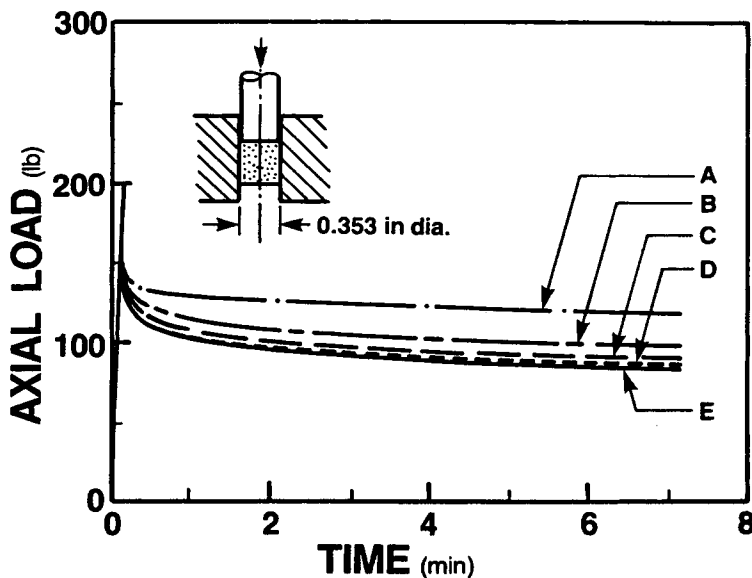


Fig. 7. Uniaxial compressive stress-relaxation behavior of the various different toners.

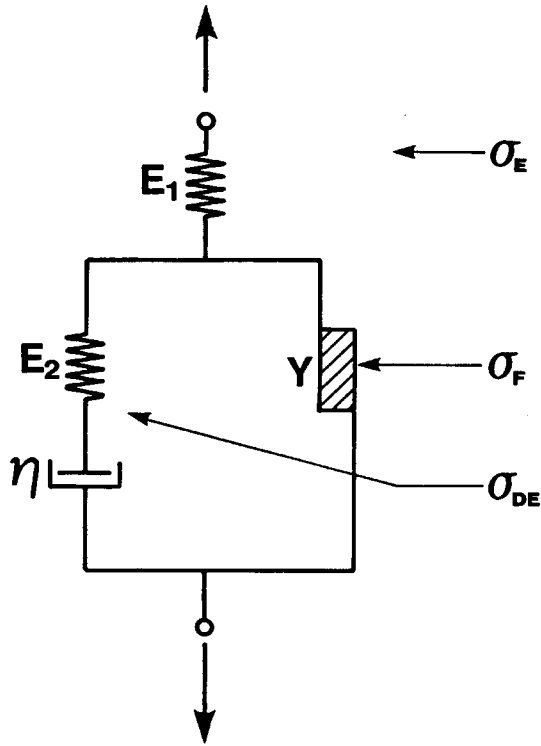


Fig. 8. The one-dimensional spring-dashpot-slider rheological model describing the stress-relaxation behavior for toners A and C.

In one such one-dimensional rheological model, Figure 8, the stress $\sigma(t)$ at any given time t can be expressed as:¹²

$$\sigma(t) = Y + \int_{-\infty}^t \frac{E_2}{1 + (E_2/E_1)} e^{-k/\tau} d\gamma$$

where

E_1, E_2 = Spring constants of the two springs

η = Viscosity of the dashpot

Y = "Yield stress" of the slider element

τ = Relaxation time

$$= \frac{1/E_1 + 1/E_2}{1/\eta}$$

γ = Total strain

Thus, the relaxation time of such a model can be obtained from a plot of $\log(\sigma - Y)$ vs. t .

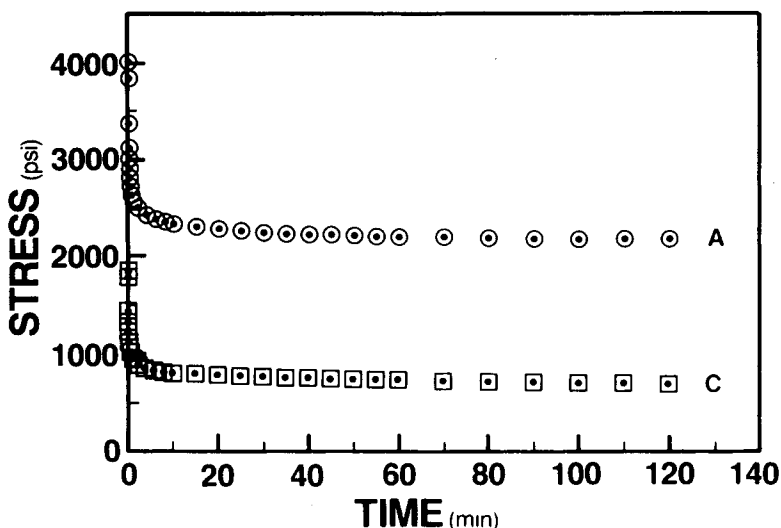


Fig. 9. The 2-hour stress-relaxation behavior of different toners.

Figure 9 shows the 2-hour stress-relaxation data for the two representative toner samples, the heat-fusing toner A and the pressure-fusing toner C. As can be seen from these data, there are substantial differences between the two toners, arising mainly from the differences in the mechanical behavior of the base resins employed. For instance, the stress values at any given time are much larger for toner A than for toner C, consistent with the fact that toner A is much stiffer and stronger than toner C.

The data of Figure 9 are replotted in Figure 10 in the form of $\log(\sigma - Y)$ vs. t plot. The Y values for the two toners were estimated from the 24-hour stress-relaxation data. Interestingly, this plot indicates the possibility of adequately characterizing some of these toners by a few predominant, discrete relaxation times, instead of the continuous relaxation spectrum. However, more numerous data need to be generated on different toners before this result can be confirmed and the discrete relaxation times assigned to the toners.

THE EFFECT OF VARYING MAGNETITE CONTENT ON THE STRESS-RELAXATION BEHAVIOR OF TONERS

The effect of varying the magnetic pigment loading from 35 to 65 wt% on the stress-relaxation behavior of type C pressure-fusing toner is shown in Figure 11. Again, among other things, the reinforcement effect caused by the magnetic pigment filler is quite apparent. More interesting features become apparent in analyzing these data in terms of the mechanical model introduced in the last section. Figure 12 shows the $\log(\sigma - Y)$ vs. t plot for the three different toners with 35, 55, and 65 wt% magnetic pigment loading. As pointed out earlier, it again appears that one may be able to characterize these toners by a few predominant relaxation times. But, more interestingly, the three curves in Figure 10 superimpose, that is, varying the magnetic pigment loading from 35 to 65 wt% does not appear to change the magnitude of the relaxation times. The effect of the magnetic pigment loading appears in the

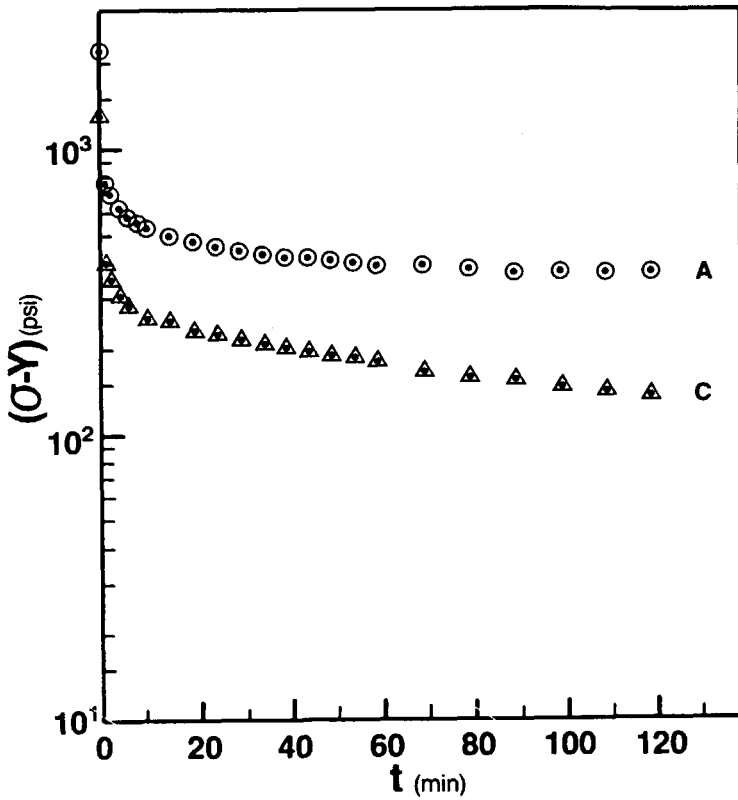


Fig. 10. Variation of $\log(\sigma - Y)$ vs. time for toners A and C.

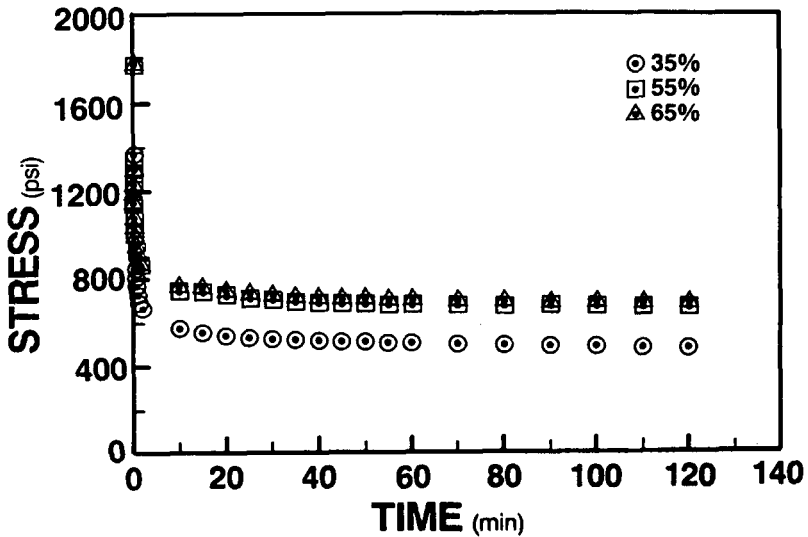


Fig. 11. Effect of the magnetic pigment loading on the 2-hour stress-relaxation data for type C toner.

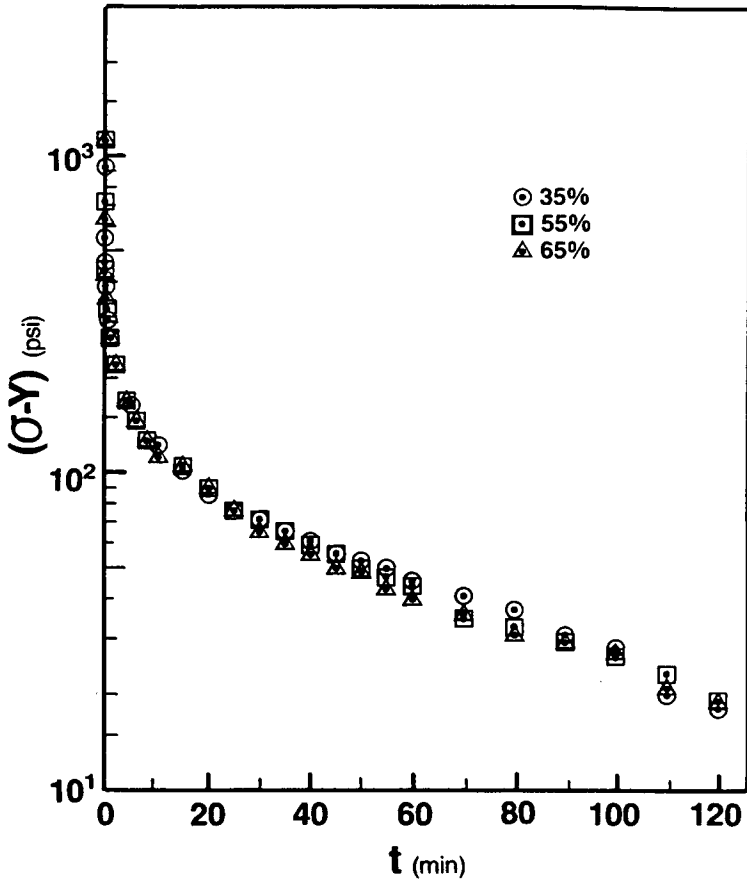


Fig. 12. Variation of $\log(\sigma - Y)$ vs. time for the three toners with 35, 55, and 65 wt% magnetic pigment loading.

differences in the yield stress values only. This results implies that at these pigment loadings, the test measures the relaxation of the base resin itself.

CONCLUSIONS

These (admittedly preliminary) results demonstrate that useful rheological data can be obtained directly upon polymer powder without the need to compression mold them into solid test specimens. This has a number of advantages quite apart from convenience. No risk is taken of changing the specimen (e.g., by recrystallizing it) and the results may be directly relevant to the end use, as in the case of the monocomponent toner powder studied in this paper.

Concerning toners, we have shown that different monocomponent toner powders can be distinguished using two simple tests, namely, a compression test and a stress-relaxation test. The relative capacities of the toners for plastic deformation and elastic recovery have been assessed (the latter in terms of stress relaxation). A mechanical spring-dashpot-slider model appears to fit the stress-relaxation data for toners with different levels of magnetic

pigment filler. The data suggest that a small number of discrete relaxation times is sufficient to characterize the time dependence.

The authors would like to thank R. H. Helland for providing a number of different toner samples and R. H. Helland, S. B. Collins, and T. J. Evensen for many helpful comments. Thanks are due to Dr. P. G. Gertenback for his constant support and encouragement and to Laura Paasch for her patience in typing the manuscript.

References

1. J. W. Dower, et al, "Toner and Toning: Technology Keys to Non-Impact Printing," Datek Report, Massachusetts, September 1981.
2. D. Garfinkel, "Toners: The Technological Explosion That's Shaping a \$1 Billion Industry," *Chem. Week*, January 30, 1985, p. 64.
3. R. J. Thompson, "The 3rd Annual Guide to Ribbons and Toners," Datek Publishing Company, Newtonville, Mass., June 1982.
4. P. B. Thompson, Paper presented at the IGC Conf., Miami, Jan. 1980.
5. S. B. Collins, A. C. Button, and R. H. Helland, 4th International Conf. on Electrophotography, Washington, D.C., November 1981.
6. U.S. Patents #3,788,944; 3,925,219; 3,928,656; 3,965,022; 4,356,764; 4,363,862.
7. S. K. Bhateja and J. R. Gilbert, "Pressure-Fusing Behavior of Monocomponent Toners," *J. Imaging Tech.*, **11**, 267 (1985).
8. S. K. Bhateja and J. R. Gilbert, "Pressure-Fusing of Monocomponent Toners at High Speeds," *J. Imaging Tech.*, **11**, 273 (1985).
9. T. Matsumoto, C. Hitomi, and S. Onogi, *Trans. Soc. Rheol.*, **19**, 541 (1975).
10. R. K. Schofield and G. W. Scott Blair, *Proc. Roy. Soc.*, **A138**, 707 (1932).
11. Y. Sawaragi and H. Tokamaru, *Mem. Fac. Eng., Kyoto University*, **16**, 100 (1954).
12. J. L. White, *J. Non-Newtonian Fluid Mech.*, **5**, 177 (1979).

Received June 24, 1986

Accepted September 19, 1986